Matter and Radiation at Extremes | RESEARCH ARTICLE | scitation.org/journal/mre

Scenario of a magnetic dynamo and magnetic reconnection in a plasma focus discharge

Cite as: Matter Radiat. Extremes 5, 046401 (2020); doi: 10.1063/1.5133103
Submitted: 24 October 2019 • Accepted: 22 June 2020 •
Published Online: 17 July 2020

P. Kubes,[1,a)] M. Paduch,[2] M. J. Sadowski,[2,3] J. Cikhardt,[1] D. Klir,[1] J. Kravarik,[1] R. Kwiatkowski,[3] V. Munzar,[1] K. Rezac,[1] A. Szymaszek,[2] K. Tomaszewski,[4] E. Zielinska,[2] M. Akel,[5] and B. Cikhardtova[1]

AFFILIATIONS

[1]Czech Technical University, 166-27 Prague, Czech Republic
[2]Institute of Plasma Physics and Laser Microfusion, 01-497 Warsaw, Poland
[3]National Centre for Nuclear Research, 05-400, Otwock-Świerk, Poland
[4]ACS Ltd., 01-497 Warsaw, Poland
[5]Atomic Energy Commission, P.O. Box 6091, Damascus, Syria

Note: This paper is part of the Special Issue on the 11th International Conference on Dense Z-Pinches (DZP2019).
[a)]**Author to whom correspondence should be addressed:** kubes@fel.cvut.cz

ABSTRACT

The paper discusses a possible energy transformation that leads to the acceleration of fast ions and electrons. In plasma-focus discharges that occur during deuterium filling, which have a maximum current of about 1 MA, the accelerated deuterons produce fast fusion neutrons and fast electrons hard X-ray emissions. Their total energy, which is of the order of several kilojoules, can be delivered by the discharge through a magnetic dynamo and self-organization to the ordered plasma structures that are formed in a pinch during the several hundreds of nanoseconds of the pinch implosion, stagnation, and evolution of instabilities. This energy is finally released during the decay of the ordered plasma structures in the volume between the anode face and the umbrella front of the plasma and current sheath in the form of induced electric fields that accelerate fast electrons and ions.

I. INTRODUCTION

Fusion-interest magnetized plasmas, which are produced in Z-pinch and dense plasma-focus (PF) devices,[1–10] have parameters that are convenient for the detailed study of their evolution in a millimeter scale with nanosecond resolution. This makes it possible to investigate the evolution of the energy that is finally released during the acceleration of fast electrons and ions. Many experiments on the energy transformation in deuterium filling have been performed within the mega-ampere PF-1000 device at the Institute of Plasma Physics and Laser Microfusion in Warsaw, Poland.[11–15] They have shown that dense toroidal and plasmoidal structures form in different experimental conditions, such as at static initial gas filling, at gas puffing, and at additional wire loads fixed along the anode axis. The forms of the observed structures have been explained as due to a flow of closed currents with toroidal and poloidal components, which can exist inside and outside the dense plasma column.

The existence of current flows and magnetic fields in the ordered plasma structures was explained based on the plasma density and plasma gradients inside the plasmoidal and toroidal structures that were calculated from the shifts of the recorded interferometric fringes using the Abel transformation.[11–15] It was shown that the density in the center of a plasmoid can reach $(4–10) \times 10^{24}$ m^{-3} and in the center of a toroid about $(1–1.5) \times 10^{24}$ m^{-3}. The plasma temperature in these situations was estimated to be on average 50 eV–75 eV.[14,15] The relaxation time, which was of the order 10 ns, resulted in a temporal quasi-equilibrium. The existence of long-lived internal plasma structures (of centimeter dimensions during about 50 ns) enabled the important simplifying assumption of quasi-stationarity to be made. In these conditions, it is possible to explain the existence of high-density gradients inside the structures analyzed using a flow of closed currents. These features observed in plasmoids might be explained by the appearance of internal currents and magnetic fields in spheromak-like structures that have toroidal and poloidal currents.[16] Such structures can exist at low β, due to the low internal plasma pressure. In the PF-1000 discharges (at $\beta \approx 1$), the dense structures considered have to expand. According to the virial theorem, as discussed in an earlier paper,[17] at equilibrium, the external pressure

should balance the mean pressure in the internal plasma region. For closed currents, the internal gradient of the plasma pressure (grad p) in quasi-stationary conditions should be equal to the internal magnetic pressure due to the current density and its magnetic field (i.e., $\mathbf{j} \times \mathbf{B}$). Consequently, the boundary of the structure should depend on the equilibrium between the external compressing pressure of the discharge current and internal repulsive pressures due to the plasma and magnetic fields. The closed currents have zero magnetic field at their surfaces. The closed magnetic fields can conserve energy, which is delivered during several hundred of nanoseconds in conditions that are convenient for the appearance of magnetic dynamo effects.[18] The spontaneous transformation of these structures can be accompanied by magnetic reconnection.[19] The acceleration of fast electrons and ions is usually correlated with the disruption of the constriction, formation, and decay of plasmoids probably containing currents in filamentary forms, which may produce local high-energy density[20] and collision-less conditions.[6] The decay of such ordered structures can lead to the fast transformation of magnetic energy into the kinetic energy of fast particles through the induction of a strong local electric field.[20] The fast deuterons are also possibly accelerated in the region surrounding the plasmoid, which has a diameter larger than the diameter of the dense pinched column.[21]

In the present work, we discuss in more detail the possible evolution of the internal magnetic fields, based on the magnetic dynamo and magnetic reconnection effects, which have generally appeared in all the experiments conducted in the PF-1000 facility. This work may help to interpret the evolution of the ordered plasma structures recorded on the interferometric and extreme ultraviolet (XUV) frames and to understand the conditions that occur during the acceleration of fast electrons and deuterons. The phases in the formation of the plasmoid, in the stagnation of the pinch column, as well as in the evolution of instabilities and secondary plasmoids followed by a decay of the dense pinch column were observed on the frames recorded for all the discharges investigated. We have estimated the currents in the toroidal tube that surrounds the dense column during the stagnation phase. The device and diagnostics used in the experiments reported are described in Sec. II. Section III describes the evolution of the currents and their internal magnetic fields in the subsequent steps of their transformation. Section IV presents the summary and conclusions.

II. DESCRIPTION OF THE DEVICE AND DIAGNOSTICS

The experiments reported were performed with the PF-1000 plasma-focus facility, which was equipped with Mather-type coaxial electrodes of length 480 mm. The anode was a thick-wall copper tube of diameter 230 mm, and the cathode of diameter 400 mm consisted of 12 stainless-steel tubes (each of diameter 82 mm). The filling pressure of the pure deuterium was 170 Pa, and the main capacitor bank (charged up to 16 kV) provided the peak current of 1.2 MA–1.3 MA.

The voltage and current-derivative waveforms, as well as the total current intensity traces, were measured at the main collector plate. Time-resolved soft X-ray (SXR) signals were recorded with a silicon p-i-n diode shielded with a Be filter of thickness 10 μm. Three scintillation detectors were used to record signals at a distance of 7 m from the focus center in the downstream (at 0°), upstream (at 180°), and side-on (at 90°) directions. These measurements allowed us to determine the instants of the emission of hard X-rays (HXRs) and fusion-produced neutrons. The mean values of the energy of the fusion neutrons and primary deuterons were determined with the time-of-flight method from the temporal difference in the amplitudes of the neutron signals recorded downstream and upstream.[22] XUV images, produced by photons with energy above 30 eV, were recorded on a four-frame micro-channel plate without a filter. Interferometric images of plasma structures were obtained with a Mach–Zehnder interferometer system with a diagnostics laser (operated at $\lambda = 527$ nm), which was equipped with appropriate optical delay lines. It was able to record 15 frames in 210 ns.[23] The lines of sight of individual interferometric beams differed by 10 mrad. The interferometer has parallel mirrors, which made it possible to record wide interferometric fringes corresponding to regions of rare plasma. The Abel transformation of the shifted interferometric fringes showed that the dense closed fringes imaged were regions with an extreme plasma density. The uncertainty due to the experimental conditions was estimated from the width of the wide fringes. Near the anode, at a radius of 2 cm–3 cm from the pinch axis, the width of the wide fringes was about 0.5 cm and corresponded to the plasma density, which was of the order of 1×10^{23} m^{-3}. That value was smaller than 10% of the plasma concentration in the plasmoidal and toroidal structures.

The total neutron yield, which was of the order of 10^{10}–10^{11}, was measured using two calibrated silver activation counters, which were placed outside the main experimental chamber. These counters were calibrated using an Am–Be source placed on the anode axis. In all cases, the maximum of the dip in the current derivative was assigned as the instant $t = 0$. This corresponded to the formation of the first plasmoid and a peak of the SXR signal. The time from the breakdown to the derivative dip was about 7 μs. The evolution of the constriction started at 50–100 ns. The formation of secondary plasmoids and the decay of the constriction was usually recorded 100 ns–200 ns after the dip. The uncertainty in the timing of different measuring channels during a single discharge was about 3 ns–5 ns.

III. EXPERIMENTAL RESULTS

A. Release of the discharge energy

The energy released in the plasma during the period Δt was calculated using the waveforms recorded for the voltage V and current I as the product $UI\Delta t$. For the average values of the voltage and current, which were 10 kV and 1 MA, respectively, it was estimated that the energy released was 100 J during each 10 ns evolution of the pinch. A higher proportion of the energy could be released during the voltage peak and the dip of the current derivative. This energy could be used to accelerate the plasma due to the Ampere force, generation of magnetic fields, and Joule heating. The Joule heating might increase the electron temperature and become lost through Bremsstrahlung radiation. The Ampere force accelerates the plasma-carrying current. The experiments described show that during the acceleration and implosion phase, only some of the discharge energy was transformed into the kinetic energy of the current sheath. Some of the energy was probably transformed into magnetic energy. The discharge current has a filamentary structure.

B. Filamentation of the current

The visible and XUV frames show that the current and the plasma sheath in many PF experiments had a filamentary character,

during both the acceleration and implosion phases.[1,24] The existence of such filaments, which have radial and azimuthal orientations, makes it possible to achieve a high energy concentration, which is important as it may be released quickly as the kinetic energy of fast particles. The presence of the filaments was also supported by observations of distinct erosion traces visible upon the anode surface after a series of PF shots.[25] The results reported in this paper show the appearance of the long-lived filaments (lasting more than 50 ns), the discrete spatial structure of the current flow through and around the dense plasma column, as well as the transport of plasma from the pinch external layers to the central region. The filamentary structures appeared to be more distinct when different admixtures of elements with higher z were used. The transformation of the current sheath into filaments in high-current Z-pinches, PF discharges, and tokamak experiments was considered by Trubnikov[26] to be a possible consequence of tearing instabilities. The fluctuations of the plasma densities, magnetic fields, and particle velocities lead to interactions between the particle beams and the surrounding plasma through the formation of magnetic shielding due to return Foucault currents. These counter-currents are surrounded by zero magnetic field and their repulsion can lead to mutual winding and the formation of helical forms. These interactions can form small "balls" of closed magnetic lines, magnetic turbulence, through reconnections of the magnetic streamlines. The current filaments can create a complicated net with axial, azimuthal, and radial components. The filaments carry currents of tens of kiloamps and have diameters of several tens of micrometers. They make it possible for the magnetic energy to become concentrated in small local regions. Their dimension corresponds to the mean free path of electron–ion and ion–ion collisions and to the Larmor radius, which results in the collision-less character of the local plasmas. The temperature inside the filaments can be higher than that in their surroundings due to Joule heating. The plasma density can be similar to that of the surrounding plasma, due to the repulsive pressure of the axial component of the internal magnetic field. Recent experiments with PF devices[27] have shown the existence, evolution, and mutual influence of the radial and azimuthal filaments.

C. Dissipation of the magnetic field

The dissipation of the magnetic field in the plasma can be characterized by the magnetic Reynolds number R_m. Its value depends on the characteristic dimensions. Macroscopic plasma structures of 1 cm scale have a high $R_m \approx 10^3$–10^4, which indicates that there is a strong frozen magnetic field with negligible dissipation for a longer time (at an electron temperature of about 50 eV above tens of microseconds). For filamentary plasma structures of size about several tens of micrometers, R_m is considerably smaller and indicates that the frozen and dissipated magnetic field components are in equilibrium. Consequently, in the filaments that exist during the acceleration and implosion of the current sheath, some of the kinetic energy (according to experimental estimations, about 50%) can be dissipated as magnetic energy. Then, the filamentary structures can explain the observed penetration of the magnetic field into the surrounding plasma in all phases of its evolution, i.e., during the motion of the current sheath, the pinch phase, the stagnation, the evolution of constrictions, and the decay of the dense pinch column.[24,28]

D. Magnetic dynamo

A magnetic dynamo together with self-organization can explain the appearance of closed components of the magnetic field in PF-1000 discharges, which were analyzed using magnetic probe measurements.[29] One possible explanation for the generation of the axial magnetic field component was made in a paper published by Mather *et al.*,[30] who suggested that there was an amplification of the geomagnetic field, but this hypothesis was not confirmed by later studies.

The generation and transformation of the magnetic field, considered in this paper as being due to a magnetic dynamo,[17] can be realized by the α effect,[18] by an increase in the magnetic energy, or by the mutual transformation of the poloidal and toroidal components of the magnetic field. The magnetic dynamo can transform the kinetic energy into magnetic energy during the perpendicular motion of the plasma across the magnetic field lines. It can also lead to the formation of a ball of magnetic field lines. The motion of the plasma stream along the magnetic field lines can transform the kinetic energy into magnetic energy and transform a toroidal magnetic line into a poloidal line.[14]

The electron densities in the PF-1000 discharges were of the order of 10^{24} m^{-3}–10^{25} m^{-3}. The velocities of the plasma column transformations, as observed and described in Ref. 15, were (1–2) $\times$ 10^5 m/s. From the known plasma densities and average temperatures of 30 eV–70 eV and with the assumed quasi-equilibrium of the plasma and magnetic pressures, earlier papers[15,16] estimated that the local magnetic field could reach about 10 T and the currents about hundreds of kiloamps. An example of the relevant calculations is presented in Sec. III G.

E. Self-generation of a magnetic field during the implosion of the current sheath

The appearance of self-generated closed azimuthal currents in PF-1000 plasmas was deduced from interferometric frames recorded during the radial implosion of the dense current sheath, and particularly from the closed dense interferometric fringes that form a toroidal structure. An example is shown in Fig. Fig. 1(a).

The closed interferometric fringes show small toroidal and helical tubes formed by the dominant azimuthal current flow. This may be due to the dissipation of some current filaments, whose energy may be transformed into magnetic energy through the generation of magnetic turbulence. The turbulence develops into larger forms by spontaneous transformation accompanied by magnetic reconnections. Due to the α effect, the turbulence can induce an increase in the azimuthal current component and the corresponding poloidal magnetic field. During the acceleration and implosion of the plasma sheath, the azimuthal current can reach about 10% of the recorded axial current.[28,29] Then, the part of the discharge current that penetrates ahead of the plasma sheath can accumulate into a few toroidal or helical tubes, as one can see in Fig. 1(a).

F. Transformation at the stopping of the imploded plasma sheath

At the current derivative dip, the implosion of the plasma sheath stops, but the current continues to penetrate into the dense plasma column[28] and flow through the region very close to the z-axis, as can be deduced from the dense interferometric fringes shown in Fig. 1(c).

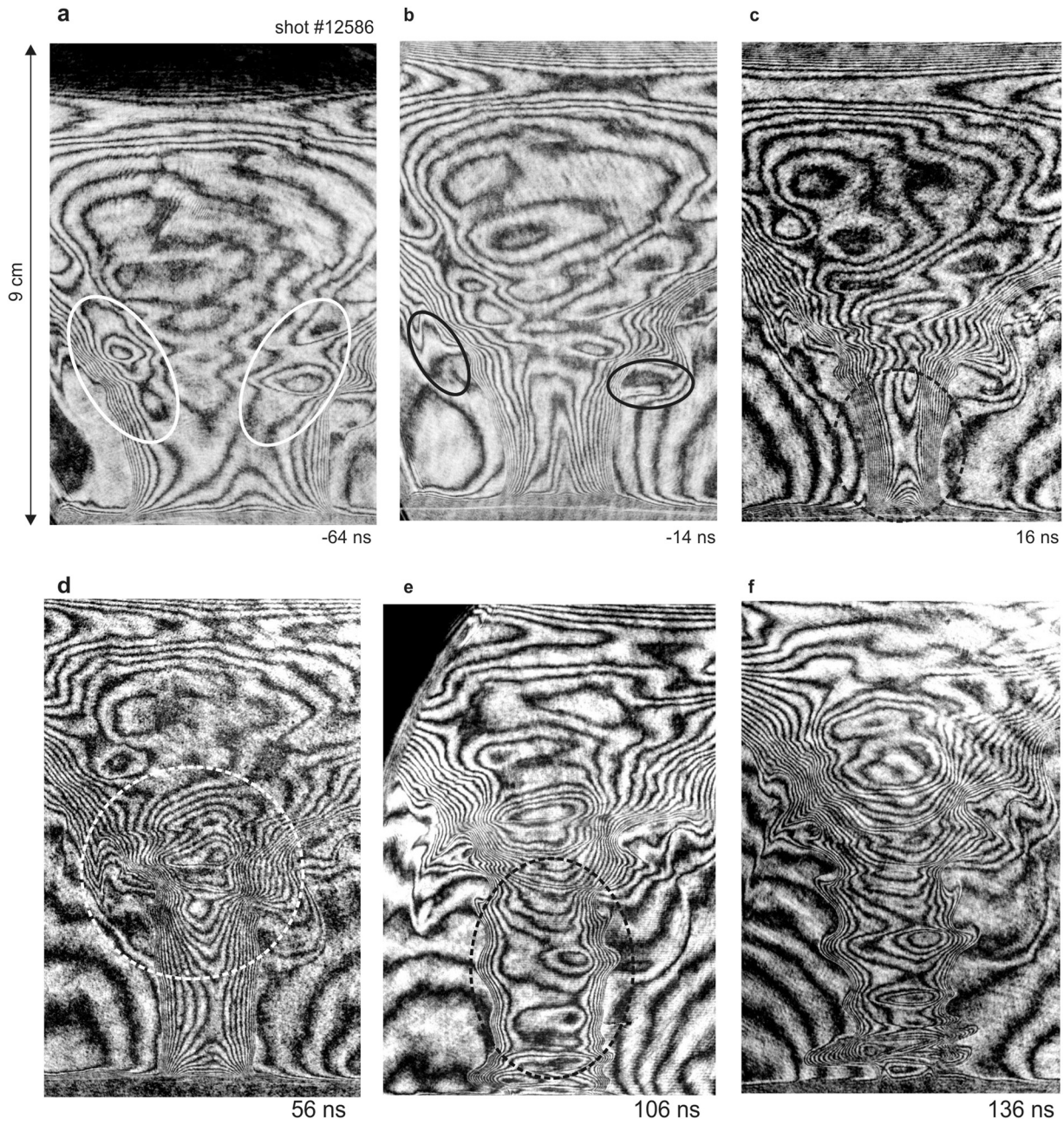

FIG. 1. Interferometric frames from shot 12 586. (a) and (b) During the implosion. (c) and (d) During the formation of the plasmoid. (e) and (f) During the stagnation phase. In (a), the internal toroidal structures are within the solid white ellipses. In (b), the external toroidal structures are within the solid black ellipses. In (c), the maximal axial current flow in the column occurs within the dashed black ellipse. In (d), the internal plasmoidal structure is within the white dashed ellipse. In (e), the phase of the pinch column with rare fringes in its interior is within the black dashed ellipse.

The plasma column has the smallest diameter first near the anode end, and then the pinching extends in the z direction due to the zippering effect. Subsequently, the plasma from the central column region near the anode end is forced to move into the region of the upper plasma lobules, which have a toroidal internal closed current. The α effect results in the formation of, first, the upper half and then later the bottom part of the plasmoid, which is marked by a white dashed ellipse in Fig. 1(d). Then, the energy of about several tens of joules from the total column volume can become concentrated in the first long-lived plasmoid, which lasts for several tens of nanoseconds. In

this phase, the closed current can also exist outside the dense column.[14] The current can flow through the surface of the dense pinch column, through the internal boundary of the plasma lobules, and come back to the anode from the lobule top through the rare plasma region. This current could also have a closed toroidal component. Both current components shift the discharge current away from the z-axis,[14,31] where a thin layer of counter-currents form.

The initial phase of this toroidal-like tube formation is marked in Fig. 1(b) by the black ellipses. The dimensions of this toroidal structure continuously increase. Note that this closed structure, which formed during the implosion of the plasma sheath, could contain the magnetic energy of the poloidal and toroidal current components.

The axial plasma transport in the dense pinch column, which results in the stagnation and the plasmoid, may be caused by the

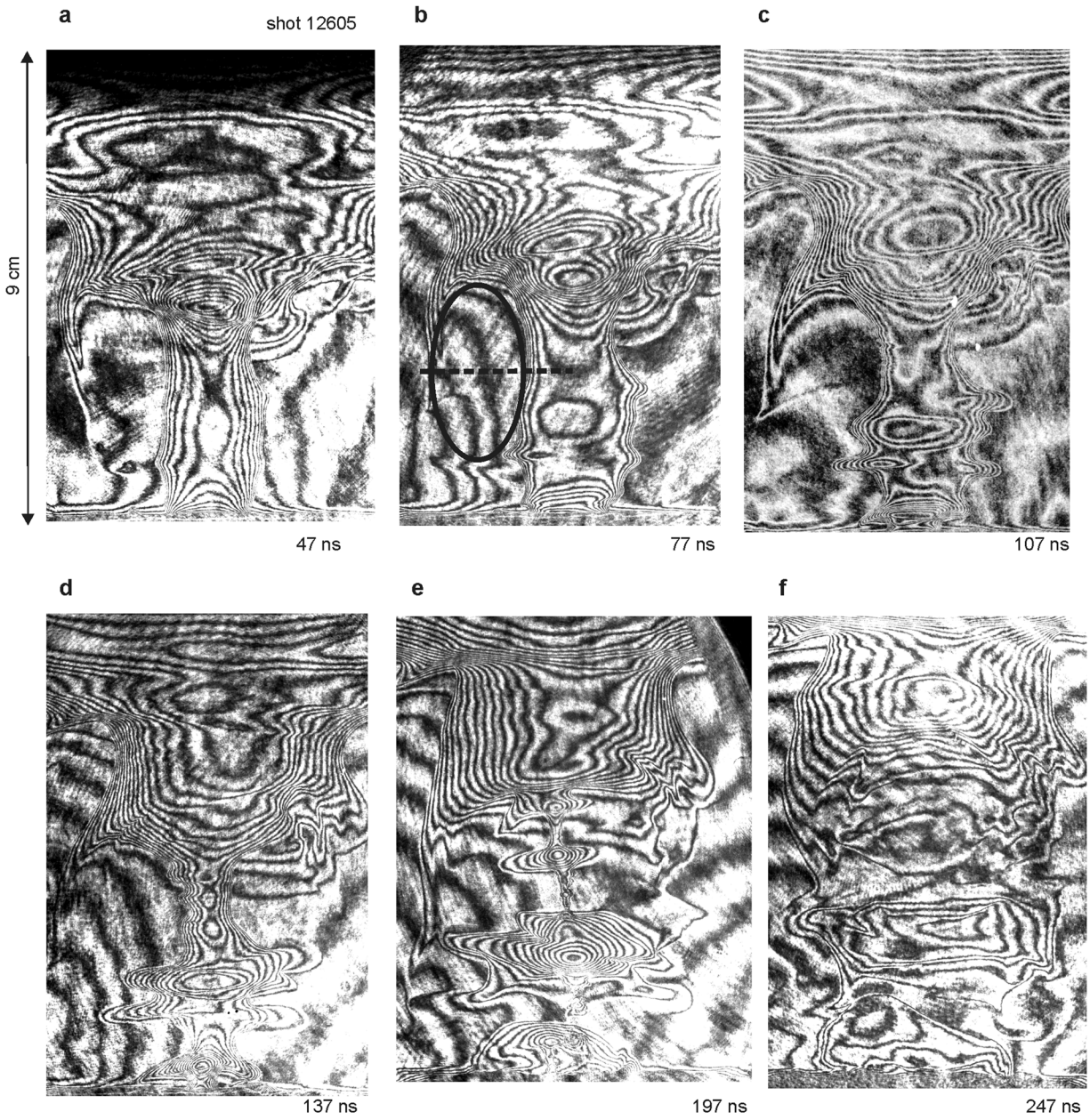

FIG. 2. Interferometric frames from shot 12 605 recorded at different phases: [(a) and (b)] During the pinch stagnation. [(c), (d), and (e)] During the evolution of the constrictions. [(e) and (f)] During the decay of the plasma column structures. In (b), the black ellipse marks the profile of the toroidal tube and the dashed black line is the cross section that was used to calculate the closed currents.

higher magnetic pressure of the increasing azimuthal current in this part of the column boundary. Some estimates for the pressures and currents are presented in Sec. III G. The axial plasma transport may be an example of the transport of magnetic energy from the discharge current to the external pinch regions, the dense plasma column, and finally to the internal plasmoids.

G. Stagnation phase

During the stagnation phase [Figs. 1(e) and 2(b)], the bottom part of the plasma column was characterized by widely spaced interferometric fringes. The upper part had the first internal plasmoid surrounded by a distinct plasma lobule. We have assumed that the plasmoid was compressed radially by the external pinch current and axially by the poloidal magnetic field that was induced by the azimuthal component of the closed current, which flowed through this part of the column boundary, as mentioned in Ref. 14 and Sec. III F, and shown in the helical structure in Fig. 3. The bottom part of the pinch column, which has radius R, did not have numerous axial interferometric fringes between the anode end and the plasmoid. The pressure in the bottom part of the pinch column was estimated by assuming that there was equilibrium between the pinching pressure p_c (originating from the poloidal current component I_p and its magnetic field B_t) and the repulsive pressure p_r (which is the sum of the difference of the mean plasma pressures $p_p \approx 2\Delta n_e kT$ and the magnetic pressure of the toroidal current component I_t and its magnetic field B_p). For quantitative estimates, we used the known relation:

$$p_r = {B_p}^2/2\mu + 2\Delta n_e kT = \sum \left(\mu I_t/2r\right) 2\mu/2\Delta n_e kT = p_c$$

$$= {B_t}^2/\mu = \sum \left(\mu I_p/2\pi R\right)^2/2\mu \qquad (1)$$

To estimate the currents and magnetic fields, we used the cross section [dashed line in Fig. 2(b)] of the closed toroidal tube marked by the black ellipse. We estimated the radial distribution of the interferometric fringes [Fig. 4(a)], the electron densities from the Abel transformation of the fringe shifts [Fig. 4(b)], and the magnetic and plasma pressures [Fig. 4(c)]. Equation (1) was used both for the current double layer and for the surface of the dense plasma column. The double layer, which has radius $R \approx 2.5$ cm, was compressed by the pressure $p_c \approx 2.5 \times 10^7$ Pa of the external discharge current, for which we used $I_p \approx 700$ kA. The pressure B_t^2/μ due to the curvature of the magnetic lines was reduced by the repulsive pressure of the plasma $p_p \approx 2 \times 10^6$ Pa, for $\Delta n_e \approx 1 \times 10^{23}$ m^{-3} and $T \approx 50$ eV [Fig. 4(c)]. Then, the remainder of the pinching pressure component, about 2.3×10^7 Pa, increased at the dense column, which has a radius of 9 mm, to $p_c \approx 17.7 \times 10^7$ Pa. The mean plasma density in the column $n_e \approx 1.6 \times 10^{24}$ m^{-3} exceeded the external plasma density $n_e \approx 3 \times 10^{23}$ m^{-3} by about $\Delta n_e \approx 1.3 \times 10^{24}$ m^{-3} and produced the plasma pressure $p_p \approx 2.1 \times 10^7$ Pa. Then, the remaining compressing pressure $p_c \approx 15.6 \times 10^7$ Pa. The poloidal magnetic field in the dense column was produced by the toroidal current flowing along the surface of the tube, for which $r \approx (25–9)/2 = 8$ mm. In the dense plasma column, $B_p \approx \mu I_t/2r$. The pinching pressure at the tube surface was balanced by the repulsive pressure of the toroidal magnetic field $B_t^2/2\mu$. The repulsive pressure also decreased the pinch pressure of the discharge current inside the dense plasma column. Then, at the surface of the dense column, the remainder of the pinching pressure was equal to the repulsive pressure B_p, the value of which was 15.6×10^7 Pa. This value was used to estimate the toroidal current component $I_t \approx 255$ kA, the poloidal magnetic field $B_p \approx 14.1$ T, the toroidal magnetic field $B_t \approx 18$ T, 7 T, and the poloidal current component $I_p \approx 640$ kA. The radial distributions of the compressive and repulsive magnetic fields are presented in Fig. 4(c). The uncertainty was estimated to be about 30%, which was caused mainly by the range of the plasma temperature and by the asymmetry of the plasma column considered for the Abel transformation.

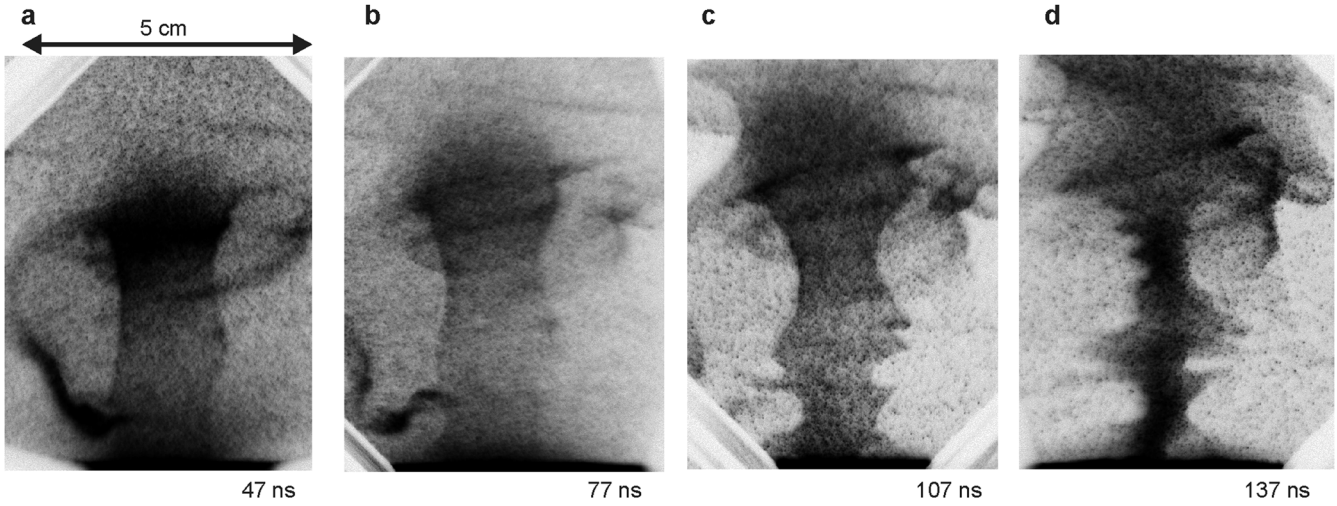

FIG. 3. XUV frames from shot 12 605 for the same discharge shown in the interferometric images in Fig. 2. These were recorded at different phases: [(a) and (b)] During the pinch stagnation. [(c) and (d)] During the evolution of the pinch constrictions. These frames, unlike the interferometric images, show distinct helical structures at the surface of the dense plasma column and at the lobule top, which can be explained by an increase in the toroidal component after the pinch stagnation.

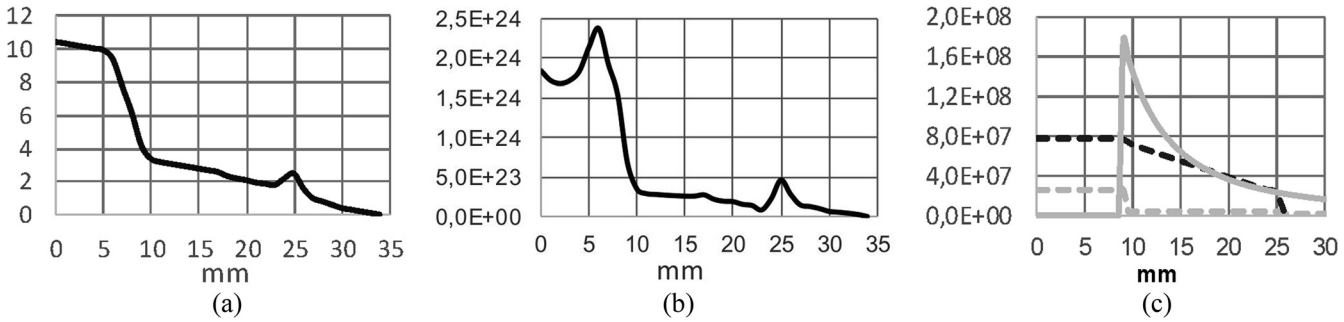

FIG. 4. Computation results: (a) Radial distribution of the interferometric fringes along the line of the cross section marked in Fig. 2(b). (b) Radial distribution of the electron density calculated from the Abel transformation of the data shown in (a). (c) Distribution of the plasma pressure (dashed black line) and the magnetic pressure associated with the pinching poloidal current I_p (full gray line) and the repulsive toroidal current I_t (dashed gray line).

Considering both magnetic field components, the ratio of the plasma and magnetic pressures β in that case was about 1. The final current $I_t \approx 180$ kA was larger than the initial current of about 70 kA ≈ 10% of I_z, evidently due to the self-generation effect. The total energy, which was contained in a volume of diameter 2 cm, could reach kilojoules.

H. Evolution of constriction and secondary plasmoids

In the final phases of the pinch stagnation in PF-1000 discharges, one can usually observe some stratification on the surface of the plasma column, as shown in Figs. 1(f) and 2(c). The dense pinched column then splits along its length into narrow and wide blocks, due to the Rayleigh–Taylor $m = 0$ instability. Subsequently, the narrow blocks implode to form constrictions. Their plasma is pushed toward the wider ends, where initially some toroids and later plasmoids are formed [Figs. 2(c) and 2(d)].[14,15] The azimuthal current in the column boundary layer increases after the pinch stagnation. This transformation corresponds with the increase in the helicity of the plasma surface visible on the XUV frames presented in Fig. 3. Later, this component penetrates into the dense plasma column, where it forms toroidal structures with larger diameters. This penetrating current may be replaced at the column boundary layer by the increasing poloidal current component dissipating from the main discharge current. Higher values of this current induce the implosion of the constrictions. The interferometric images show that this compression is not adiabatic and that its plasma is injected into the secondary plasmoids. These plasmoids differ from the first internal plasmoid because they have a shorter life-time due to the smaller toroidal current component, which can be insufficient to maintain its pressure equilibrium for a longer time (tens of nanoseconds). In general, the plasma region can undergo compression by the pinch effect in the axial region of the plasmoid. Then, the secondary plasmoids can absorb the kinetic energy from the plasma flowing from the constrictions. This energy is transformed into magnetic energy due to the α effect described above. Consequently, during this phase, the magnetic energy can increase considerably in the dense plasma column and in its surroundings.

I. Release of the magnetic energy and acceleration of fast electrons and ions

The dominant HXR and neutron production usually starts during the decay of the plasmoids and the disruption of the constriction. The narrow constriction often decays axially when it is absorbed into the secondary plasmoids or by the formation of new third-generation plasmoids, as one can see in Fig. 2(e). The zippering of the column along its length leads to the temporal evolution of the final phase, in which there are a few constrictions on top of each other [Fig. 2(e)]. The plasmoids decay when their centers explode and their boundaries expand. Then, some of the magnetic energy conserved in the closed internal and external structures can accelerate fast particles.[14,15] The release of the magnetic energy can also proceed by magnetic reconnections during the spontaneous coalescence of two parallel filaments, in which the decaying magnetic field induces a strong electric field.[18]

The tracks of fast deuterons recorded end on[21] show that they originate from several rings with diameters ranging up to 20 cm, i.e., practically from the whole surface of the anode face. These ring sources support the existence of several layers of closed currents and the shift of the discharge current toward the edge of the anode face. It also indicates that these structures exist in a larger volume outside the viewing field of the interferometer system.

The length of the plasma column usually increases linearly with the volume of the closed currents. The magnetic field B decreases as $1/r$ (at the radial distribution of that), and when the current is 1 MA, it reached $B \approx 0.2/r$, where r is the radius expressed in meters. Then, the magnetic energy also increases linearly with r, and its total value in the volume above the anode front can reach several kilojoules (for several hundreds of nanoseconds). This energy can be contained in the closed local magnetic fields and it can be released as energetic particle beams, which are emitted from the plasma column (mainly during its decay), as well as from its surroundings.

This energy of about several kilojoules was estimated from the measured neutron yield, the mean energy of the accelerated fast deuterons, the cross section of D–D fusion reactions for this deuteron energy, and the known density of the dense plasma at the top of the dense pinch column. The mean energy of fast deuterons was estimated from the temporal differences in the neutron signals recorded in the downstream and upstream directions. The mean energy can reach 5 kJ. The detailed calculations were presented in an earlier paper.[32]

Characteristic waveforms and fast neutron signals were recorded for almost all investigated PF-1000 discharges. Some examples are presented in Figs. 5 and 6.

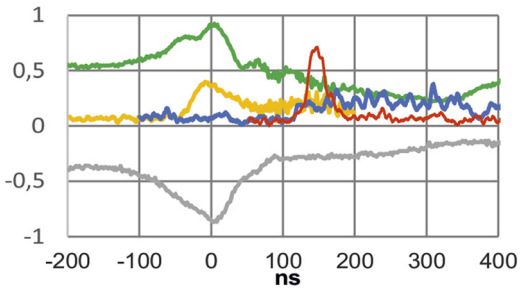

FIG. 5. Waveforms from shot 12 605. Gray: The current derivative with a dip. Green: Voltage with a peak at the smallest pinch diameter. Yellow: SXR pulses emitted at the current derivative dip, at the voltage peaks, and at the formation of the first plasmoid. Red: HXR signal. Blue: Neutrons at 2.45 MeV shifted in time. The neutrons begin to be emitted during the disruption of the constriction [Fig. 2(e)]. The SXRs increase during the transformation of the kinetic energy into heat.

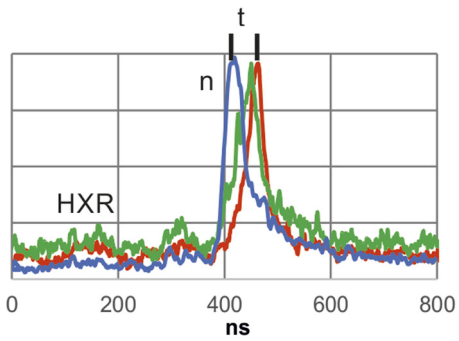

FIG. 6. Neutron signals recorded at a distance of 7 m in the downstream (blue), side-on (green), and upstream (red) directions. The temporal shift of the peaks (t) made it possible to calculate the dominant neutron velocity (downstream and upstream) and the mean energy E_d of the deuterons producing the fusion neutrons. In this shot, it was estimated that $E_d \approx 100$ keV at $t \approx 50$ ns. In all these PF-1000 shots, E_d reached values of 70 keV–500 keV. At the mean deuteron energy of 200 keV, the increase in the FWHM of the neutron pulse (measured at 7 m) was about 20 ns.

J. Discussion on the acceleration of fast deuterons

Schmidt *et al.*[33] described fully kinetic particle-in-cell simulations of a megajoule dense PF experiment. The total neutron yield, the duration of neutron production, and the energy distribution from this modeling are consistent with the experimental results from the PF-1000 facility. The authors of that paper assumed that the mechanism of the deuteron acceleration is connected with the anomalous resistance. We also compared the distributions of the plasma density and the neutron production processes. In the fully kinetic model, the maximum neutron production corresponds to the maximum constriction. Small sources of fast particles can be distributed along the boundary of the dense plasma column, mainly in a region with radius from 2 mm to 5 mm. The acceleration of the charged particles is probably caused by local electric fields, which can form in the low-density regions between dense fingers corresponding to the Rayleigh–Taylor instabilities. In the PF-1000 facility, the dominant neutron production is correlated with a disruption of the pinch constriction and a decay of the ordered plasma structures. The acceleration of the charged particles can be explained by a release of the magnetic energy from these structures in regions extending to a radius of a few centimeters. This requires further research.

A possible explanation for the formation of the organized plasma structures is described in a new paper.[34] It presents a qualitative model that can describe the magnetic fields associated with the organized structures, which supports the supposition that they play a crucial role in the production of fusion neutrons in PF discharges.

Recently, the ion acceleration mechanism has been studied in detail during experiments performed with the GIT-12 generator. Deuterium gas-puffed Z-pinch discharges produced ions with energies of up to 30 MeV.[10] The off-axis ion emission was recorded from local sources distributed along concentric circles and radial lines. The main acceleration occurred during the strong $m = 0$ instabilities. The acceleration of the deuterons, which had energies >20 MeV, was explained by an increase in the Z-pinch impedance (>10 Ω) with a sub-nanosecond decay time. The high voltage peak could be driven by the inductive energy, which is stored around the Z-pinch column and which can be released during a sub-nanosecond current drop. This behavior can be characterized as the formation of a high-density plasma diode with a microsecond conduction time, nanosecond opening switch, and a high voltage multiplication (even up to 50 times). This mechanism can produce ions with energies of tens of mega-electronvolts, which can penetrate even high-density plasmas. The ion energies mentioned above differ by about two orders of magnitude from those measured in the PF-1000 discharges, but some experimental results are similar, e.g., the dominant acceleration of fast particles after the pinch disruption, as well as the radial and azimuthal distribution of fast deuteron sources, which were also observed in a region surrounding the dense plasma column. Further research may provide information to support or refute these physical models.

IV. SUMMARY

In this paper, we presented the transformations of plasma energy during the evolution of the ordered plasma structures that are visible in interferometric frames. The magnetic dynamo effect is a possible mechanism. The α effect may occur during fluctuations of plasma densities and velocities, as well as changes in the local magnetic fields of the current filaments, which have diameters of several tens of micrometers. At this scale, the plasma is collision-less and the magnetic Reynolds number is close to 1, which allows the magnetic energy to dissipate quickly. During this transformation, plasma streams can interact with the magnetic field to form magnetic turbulence, which can spontaneously generate, through magnetic reconnections, ordered plasma structures with closed internal currents and corresponding magnetic fields. An example was calculated from the distribution of the electron densities during the stagnation phase. This process can accumulate an energy of several kilojoules in the plasma volume in front of the anode. Most of this energy can subsequently be released from this volume in a relatively short time of several tens of nanoseconds in the form of the observed HXR and fusion neutrons.

The results presented are evidently qualitative. Their verification and a more exact quantitative description of the energy transfer needs further experimental studies supported by appropriate numerical simulations.

ACKNOWLEDGMENTS

This study was supported in part by research programs funded by Grant Nos. MSMT LTT17015, LTAUSA17084, CZ.02.1.01/0.0/0.0/16_019/0000778, GACR 19-02545S, PPN/BIL/2018/00133/U/00001, IAEA CRP 23071, CRP 23225, and SGS 19/167/OHK3/3T/13, as well by the Polish Ministry of Science and Higher Education using the financial resources allocated in 2019 for international co-financed projects.

REFERENCES

[1]A. Bernard, H. Bruzzone, P. Choi *et al.*, "Scientific status of plasma focus research," J. Moscow Phys. Soc. **8**, 93 (1998).

[2]L. Bertalot, H. Herold, U. Jäger *et al.*, "Mass and energy analysis and space-resolved measurements of ions from plasma focus devices," Phys. Lett. **79**, 389 (1980).

[3]A. Mozer, M. Sadowski, H. Herold *et al.*, "Experimental studies of fast deuterons, impurity- and admixture-ions emitted from a plasma focus," J. Appl. Phys. **53**, 2959 (1982).

[4]M. G. Haines, "A review of the dense Z-pinch," Plasma Phys. Controlled Fusion **53**, 093001 (2011).

[5]D. D. Ryutov, M. S. Derzon, and M. K. Matzen, "The physics of fast z pinches," Rev. Mod. Phys. **72**, 167 (2000).

[6]D. D. Ryutov, "Characterizing the plasmas of dense z-pinches," IEEE Trans. Plasma Sci. **43**, 2363 (2015).

[7]L. Soto, "New trends and future perspectives on plasma focus research," Plasma Phys. Controlled Fusion **47**, A361 (2005).

[8]V. I. Krauz, "Progress in plasma focus research and applications," Plasma Phys. Controlled Fusion **48**, B221 (2006).

[9]M. Krisnan, "The dense plasma focus: A versatile dense pinch for diverse applications," IEEE Trans. Plasma Sci. **40**, 3189 (2012).

[10]D. Klir, A. V. Shishlov, V. A. Kokshenev *et al.*, "Ion acceleration mechanism in mega-ampere gas-puff z-pinches," New J. Phys. **20**, 053064 (2018).

[11]M. Scholz, L. Karpinski, M. Paduch *et al.*, "Recent progress in 1 MJ Plasma-Focus research," Nukleonika **46**, 35 (2001).

[12]M. J. Sadowski and M. Scholz, "Results of large-scale Plasma-focus experiments and prospects for neutron yield optimization," Nukleonika **47**, 31 (2002).

[13]P. Kubes, D. Klir, J. Kravarik *et al.*, "Scenario of pinch evolution in a plasma focus discharge," Plasma Phys. Controlled Fusion **55**, 035011 (2013).

[14]P. Kubes, M. Paduch, M. J. Sadowski *et al.*, "Evolution of the pinched column during hard X-ray and neutron emission in a dense plasma focus," J. Fusion Energy **38**, 490 (2019).

[15]P. Kubes, M. Paduch, M. J. Sadowski *et al.*, "Evolution of a pinch column during the acceleration of fast electrons and deuterons in a plasma-focus discharge," IEEE Trans. Plasma Sci. **47**, 339 (2019).

[16]P. Bellan, *Spheromaks* (Imperial College Press, London, 2000).

[17]M. A. Leontovich, Voprosy teorii plazmy, Tom 2, Gosatomizdat 1963, Chapter by V. D. Shafranov, Equilibrium of plasma in magnetic field (in Russian).

[18]H. K. Moffatt, *Magnetic Field Generation in Electrically Conducting Fluids* (Cambridge University Press, 1978).

[19]M. Yamada, R. Kulsrud, and H. Ji, "Magnetic reconnection," Rev. Mod. Phys. **82**, 603 (2010).

[20]P. Kubes, M. Paduch, B. Cikhardtova *et al.*, "The influence of the nitrogen admixture on the evolution of a deuterium pinch column," Phys. Plasmas **23**, 082704 (2016).

[21]P. Kubes, M. Paduch, M. J. Sadowski *et al.*, "Features of fast deuterons emitted from plasma focus discharges," Phys. Plasmas **26**, 032702 (2019).

[22]K. Rezac, D. Klir, P. Kubes *et al.*, "Improvement of time-of-flight methods for reconstruction of neutron energy spectra from D(d,n)^{3}He fusion reactions," Plasma Phys. Controlled Fusion **54**, 105011 (2012).

[23]E. Zielinska, M. Paduch, and M. Scholz, "Sixteen-frame interferometer for a study of a pinch dynamics in PF-1000 device," Contrib. Plasma Phys. **51**, 279 (2011).

[24]W. H. Bostic, "The pinch effect revisited," Int. J. Fusion Energy **1**, 1 (1977).

[25]P. Kubes, M. Paduch, J. Cikhardt *et al.*, "Filamentation in the pinched column of the dense plasma focus," Phys. Plasmas **24**, 032706 (2017).

[26]B. A. Trubnikov, "Current filaments in plasmas," Plasma Phys. Rep. **28**, 312 (2002).

[27]E. Lerner, LPP Fusion, https://lppfusion.com/images-catch-ff-2b-in-action/, 2020.

[28]V. Krauz, K. Mitrofanov, M. Scholz *et al.*, "Experimental study of the structure of the plasma-current sheath on the PF-1000 facility," Plasma Phys. Controlled Fusion **54**, 025010 (2012).

[29]V. I. Krauz, K. N. Mitrofanov, M. Scholz *et al.*, "Experimental evidence of existence of the axial magnetic field in a plasma focus," Europhys. Lett. **98**, 045001 (2012).

[30]J. W. Mather, P. J. Bottoms, and J. P. Carpenter, "Stability of the dense plasma focus," Phys. Fluids **12**, 2343 (1969).

[31]P. Kubes, M. Paduch, M. J. Sadowski *et al.*, "External current layer of a pinch column in a dense plasma focus," Phys. Plasmas (submitted).

[32]P. Kubes, D. Klir, J. Kravarik *et al.*, "Energy transformations in column of plasma-focus discharges with megaampere currents," IEEE Trans. Plasma Sci. **40**, 481 (2012).

[33]A. Schmidt, A. Link, D. Welch *et al.*, "Fully kinetic simulations of megajoule-scale dense plasma focus," Phys. Plasmas **21**, 102703 (2014).

[34]S. K. H. Auluck, "Acceleration and trapping of fast ions in self-organized magneto-plasma structures in the dense plasma focus," Phys. Plasmas **27**, 022308 (2020).